energies

MDPI

Article

Zigzag Multirod Laser Beam Merging Approach for Brighter TEM_{00}-Mode Solar Laser Emission from a Megawatt Solar Furnace

Hugo Costa, Joana Almeida, Dawei Liang *, Miguel Catela, Dário Garcia, Bruno D. Tibúrcio and Cláudia R. Vistas

Centro de Física e Investigação Tecnológica (CEFITEC), Departamento de Física, Faculdade de Ciências e Tecnologia, Universidade NOVA de Lisboa, 2829-516 Caparica, Portugal; hf.costa@campus.fct.unl.pt (H.C.); jla@fct.unl.pt (J.A.); m.catela@campus.fct.unl.pt (M.C.); kongming.dario@gmail.com (D.G.); brunotiburcio78@gmail.com (B.D.T.); carvistas@gmail.com (C.R.V.)

* Correspondence: dl@fct.unl.pt

Abstract: An alternative multirod solar laser end-side-pumping concept, based on the megawatt solar furnace in France, is proposed to significantly improve the TEM_{00}-mode solar laser output power level and its beam brightness through a novel zigzag beam merging technique. A solar flux homogenizer was used to deliver nearly the same pump power to multiple core-doped Nd:YAG laser rods within a water-cooled pump cavity through a fused silica window. Compared to the previous multibeam solar laser station concepts for the same solar furnace, the present approach can allow the production of high-power TEM_{00}-mode solar laser beams with high beam brightness. An average of 1.06 W TEM_{00}-mode laser power was numerically extracted from each of 1657 rods, resulting in a total of 1.8 kW. More importantly, by mounting 399 rods at a 30° angle of inclination and employing the beam merging technique, a maximum of 5.2 kW total TEM_{00}-mode laser power was numerically extracted from 37 laser beams, averaging 141 W from each merged beam. The highest solar laser beam brightness figure of merit achieved was 148 W, corresponding to an improvement of 23 times in relation to the previous experimental record.

Keywords: beam merging; multirod; Nd:YAG; solar furnace; solar flux homogenizer; solar laser; TEM_{00}-mode

Citation: Costa, H.; Almeida, J.; Liang, D.; Catela, M.; Garcia, D.; Tibúrcio, B.D.; Vistas, C.R. Zigzag Multirod Laser Beam Merging Approach for Brighter TEM_{00}-Mode Solar Laser Emission from a Megawatt Solar Furnace. *Energies* **2021**, *14*, 5437. https://doi.org/10.3390/en14175437

Academic Editor: Bashir A. Arima

Received: 20 July 2021
Accepted: 30 August 2021
Published: 1 September 2021

1. Introduction

The production of coherent and narrowband laser radiation from broadband solar radiation has gained an ever-increasing importance over the years, providing cost-effective solutions to laser radiation in a more sustainable way. Powered by the largest and most exploitable renewable energy resource, solar-pumped laser systems may offer design simplicity and dismissal of artificial power generation and conditioning equipment. They are especially suited for space-based applications wherein extended run times are required and compactness, reliability, and efficiency are critical, including wireless power transmission [1], deep-space optical communications [2], laser propulsion [3], and asteroid deflection [4]. In addition, its use can be of value for terrestrial applications, in fields such as thermochemistry and materials processing [5–7].

Although the first report of a solar-pumped maser occurred in the 1960s [8], it was only in the 21st century that the most significant progress in solar laser research was made, when aiming to boost the collection efficiency [9–16]—defined as solar laser output power per unit of primary concentrator area [9]. The current record is 32.5 W/m^2, reached through end-side-pumping a single Cr:Nd:YAG ceramic rod with 4.5 mm diameter and 35 mm length, in 2018 [15]. Brightness figure of merit—given by the quotient between the output laser power and the product of the beam quality factors M_x^2 and M_y^2 [9]—is another key parameter for evaluation of the laser performance. In 2017, using a single 4-mm diameter, 35-mm length Nd:YAG rod, the experimental record of 6.46 W brightness figure of merit

was attained, as well as a 7.9 W/m^2 TEM$_{00}$-mode collection efficiency [16]. However, the exposure of a single rod to a large amount of pump power can induce excessive heat within it and, consequently, substantial thermal stress effects [17]. These effects are conducive to laser beam distortion, depolarization loss, and fracture of the laser rod, which occurs when the stress originated from the temperature gradients in the laser material surpasses its tensile length [18]. Moreover, overcoming this hindrance is of paramount importance when scaling the laser power without hampering its beam quality [19]. The reduction of the rod diameter makes it more thermally resistant and can improve considerably the beam quality, even though the laser power production could then be severely limited.

Nd:YAG is the most commonly used laser material for highly intense solar pumping in light of the appropriate spectroscopic properties of the dopant [20], and the excellent thermomechanical properties of the host material, giving it great resilience and durability [21]. Its availability and low cost compared to alternative laser materials are also factors that are taken into consideration. The Nd:YAG laser is a four-level system, as depicted by the simplified energy level diagram in Figure 1. The laser beams are typically emitted at a wavelength of 1064 nm, originated from the transition from the $^4F_{3/2}$ to the $^4I_{11/2}$ levels [18]. In a four-level laser medium, the lower laser level is well above the ground state, being quickly depopulated by multiple phonon transitions. This means that reabsorption of the laser radiation can be avoided, and a lower threshold pump power can be achieved, making it easier to obtain stimulated emission with relatively low pump power.

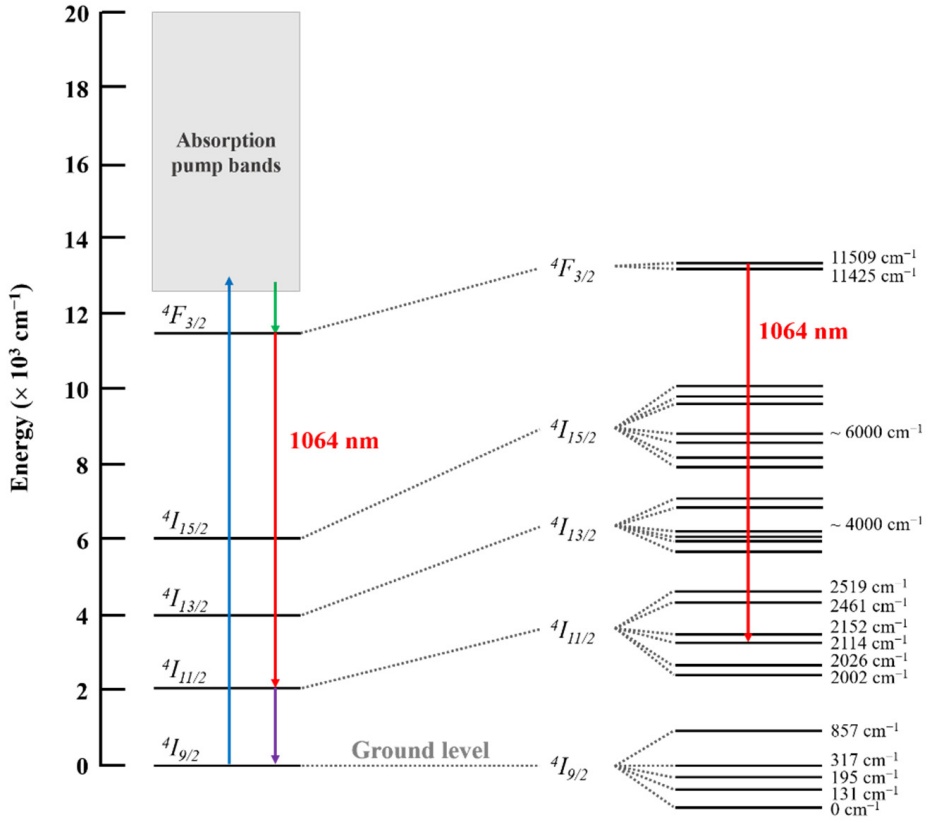

Figure 1. Simplified energy level diagram of Nd:YAG (based on [18]).

Core-doped ceramic media, which are laser active only in their core, possess a cladding around it with the same properties as the host material. The cladding can be either undoped or doped with a different material that efficiently absorbs light at the signal wavelength. This technology arose with the purpose of enhancing the brightness of diode-pumped solid-state lasers, compared to that with conventional single-crystal laser media [22,23], and has shown to be promising for solar laser research [24–27]. Since the cross-section of the laser rod is widened by the cladding, the laser active region has room for wider Gaussian

intensity distributions without truncating its wings. The upper laser level becomes even more populated than the lower level with the increase of the average intensity in the doped part of the laser rod, and a more efficient built-up inversion can be obtained. Therefore, the higher the population inversion, the more efficient the laser power production is. The impact of diffraction losses on the laser beam quality may also be diminished [22,23].

As previously mentioned, lasers are indispensable materials-processing tools, as they enable the productivity enhancement that manufacturers look for to extend their business to new segments. In recent times, this search has resulted in the simultaneous emission of several laser beams on a single workpiece, where each one could be optimized to perform only a part of the overall process [28]. It has proven its effectiveness in applications such as welding, brazing, surface texturing [28], microstructuring [29], laser ablation, drilling, and cutting [30,31], achieving more positive outcomes compared to that with the conventional single laser beam. In similar fashion, researchers have been proposing concepts based on the distribution of concentrated radiation among multiple rods [32–39] to abate the thermal stress effects. Through numerical work, multirod laser stations have shown great potential to be used in megawatt solar furnaces (MWSF) [32,36,38]. For the MWSF of Procédés, Matériaux et Energie Solaire—Centre National de la Recherche Scientifique (PROMES-CNRS), total multimode solar laser power of 22.84 kW was numerically attained from a side-pumping laser system with a solar flux homogenizer and 12 Nd:YAG rods of 10 mm diameter and 516 mm length, resulting in 12.48 W/m^2 collection and 2.28% solar-to-laser power conversion efficiencies [36]. This concept, however, displayed strong thermal lensing in each rod, impairing the laser beam quality. In consideration of this, a 32-rod side-pumping scheme was proposed for that same facility [38]. With rods of 6 mm diameter and eight different lengths, it showed a considerable alleviation of the thermal lensing effects and improvement of the laser beam quality factors, possibly enabling the generation of 9.44 kW total laser power from 32 laser beams with quasi-Gaussian profiles. Nevertheless, in both these schemes, the thermal lensing was still very pronounced in the large diameter rods, so operating with rods with smaller diameter was not possible. The maximum extraction of TEM_{00}-mode solar laser is only conceivable by adopting laser rods of small diameter and resonator configurations of large-mode volume, which leads to a substantial improvement of the laser beam quality [16,40–44]. Gaussian TEM_{00}-mode laser beams are desired for many applications due to having the lowest divergence and, consequently, the highest intensity and brightness, allowing greater energy concentration for long distances [18]. This type of laser beam is typically used in materials processing as a result of the preservation of its shape when passing through an optical system consisting of multiple elements employed to guide the laser radiation to the workpiece [45]. These features, coupled with the possibility to be focused to a diffraction-limited spot, make TEM_{00}-mode laser beams the best option for microfabrication applications [45], for example. Moreover, by making use of a laser beam merging technique, TEM_{00}-mode laser beams of higher power, enhanced beam quality and, thus, higher brightness can be obtained [46].

In that regard, an alternative multirod end-side-pumping concept is proposed to significantly improve the TEM_{00}-mode solar laser output power level and its beam brightness through a novel zigzag multirod laser beam merging technique. It comprised of the MWSF of PROMES-CNRS for collection and concentration of solar light, a solar flux homogenizer with hexagonal shaped faces, and multiple arrays of core-doped Nd-YAG rods placed after a fused silica window at the homogenizer's output face. Surrounding these rods is a hexagonal shaped pump cavity, used to help in providing approximately the same amount of solar power to pump each rod. All of the design parameters of the present approach were numerically optimized on both Zemax® nonsequential ray-tracing and laser cavity analysis and design (LASCAD™) software.

2. Description of the Multibeam Solar Laser Station

2.1. Megawatt Solar Furnace of PROMES-CNRS

The MWSF of the PROMES-CNRS laboratory (Figure 2), in Odeillo, France, is comprised of a 63-heliostat field with a total surface area of 2835 m^2 and a 1830 m^2 facetted truncated parabolic mirror with 18 m focal length, mounted on the north face of an eight-story building [47]. The 63 heliostats are distributed among eight flat terraces at different heights, placed in staggered rows (Figure 2c). Each heliostat tracks the Sun, collects the solar rays and redirects them horizontally toward the parabolic mirror. It then focuses 1 MW of solar power into an 80 cm diameter Gaussian spot, reaching a peak flux value beyond 10 W/mm^2 [48]. The light source in Zemax® was programmed accordingly for the design and optimization of the multirod end-side-pumping concept, by manually adjusting the G_X and G_Y parameters, which represent the Gaussian distribution parameters in the *x*- and *y*-axes. The desired light distribution at the focus was attained at $G_X = G_Y = 29{,}000$.

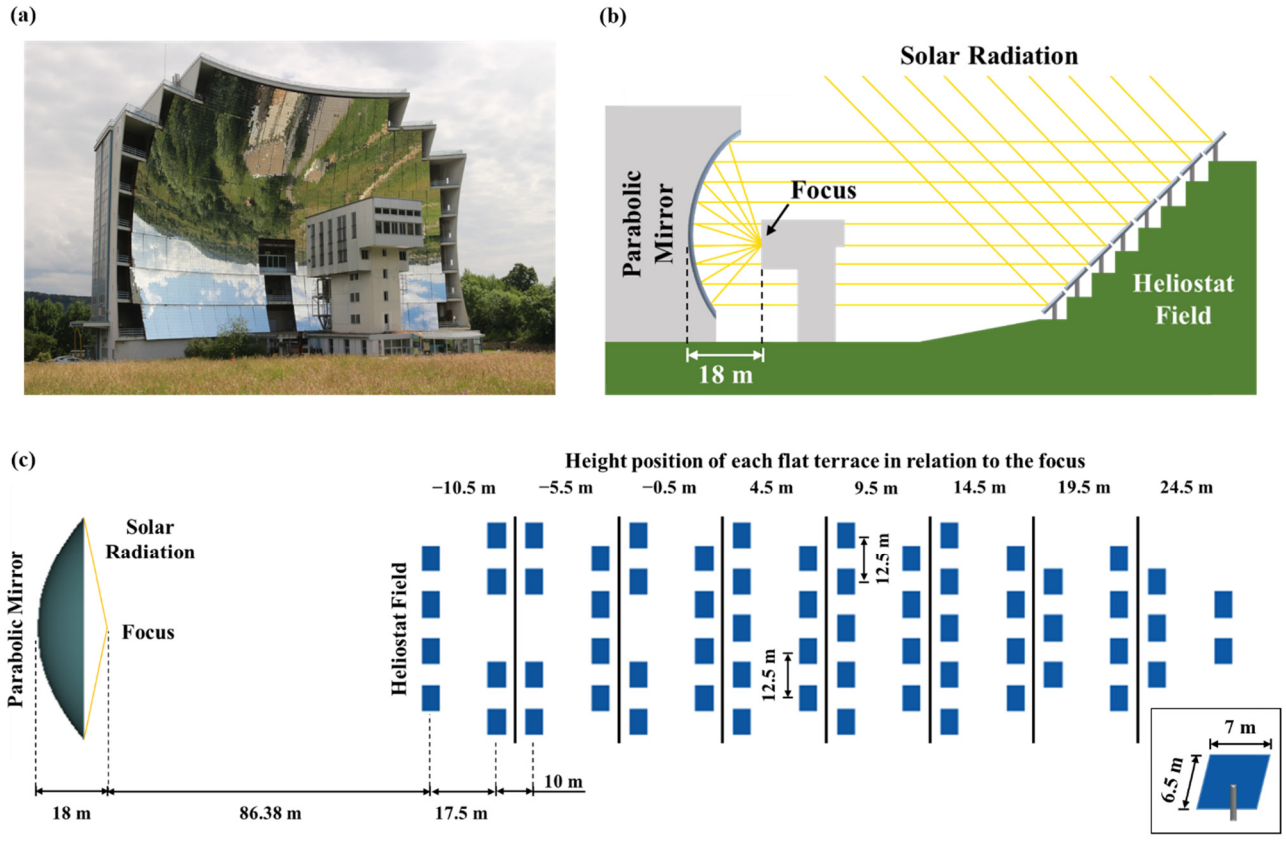

Figure 2. (**a**) Photograph and (**b**) simplified schematic of the MWSF facility in Odeillo, France. (**c**) Top-view of the solar energy collection and concentration system (based on [47]). The dimensions of a heliostat are presented in the inset of (**c**).

2.2. Solar Flux Homogenizer and Arrays of Core-Doped Nd:YAG Rods

The concentrated solar radiation from the parabolic mirror was received by a hollow homogenizer, with hexagonal input and output faces, placed at the focal zone (Figure 3a). Its role was to reshape the Gaussian solar pump light distribution at its input face into a nearly uniform one at its output end. Both end faces of the homogenizer were designed to present an apothem of 203 mm, while a 390 mm length was necessary to attain the desired type of solar pump light distribution at the exit. An inner wall reflectivity of 98% and an active back-face water cooling of the homogenizer were considered.

As depicted in Figure 3a, at the homogenizer's input face, the concentrated solar radiation presented a Gaussian distribution with a 10.21 W/mm^2 peak flux. The solar rays underwent multiple reflections along its length, and a nearly uniform profile with an average flux of 4.38 W/mm^2 was achieved at the output end, after which a thin hexagonal

fused silica window was positioned. At the input/output face of the homogenizer, a solar rays' rim angle of nearly 80° was also found.

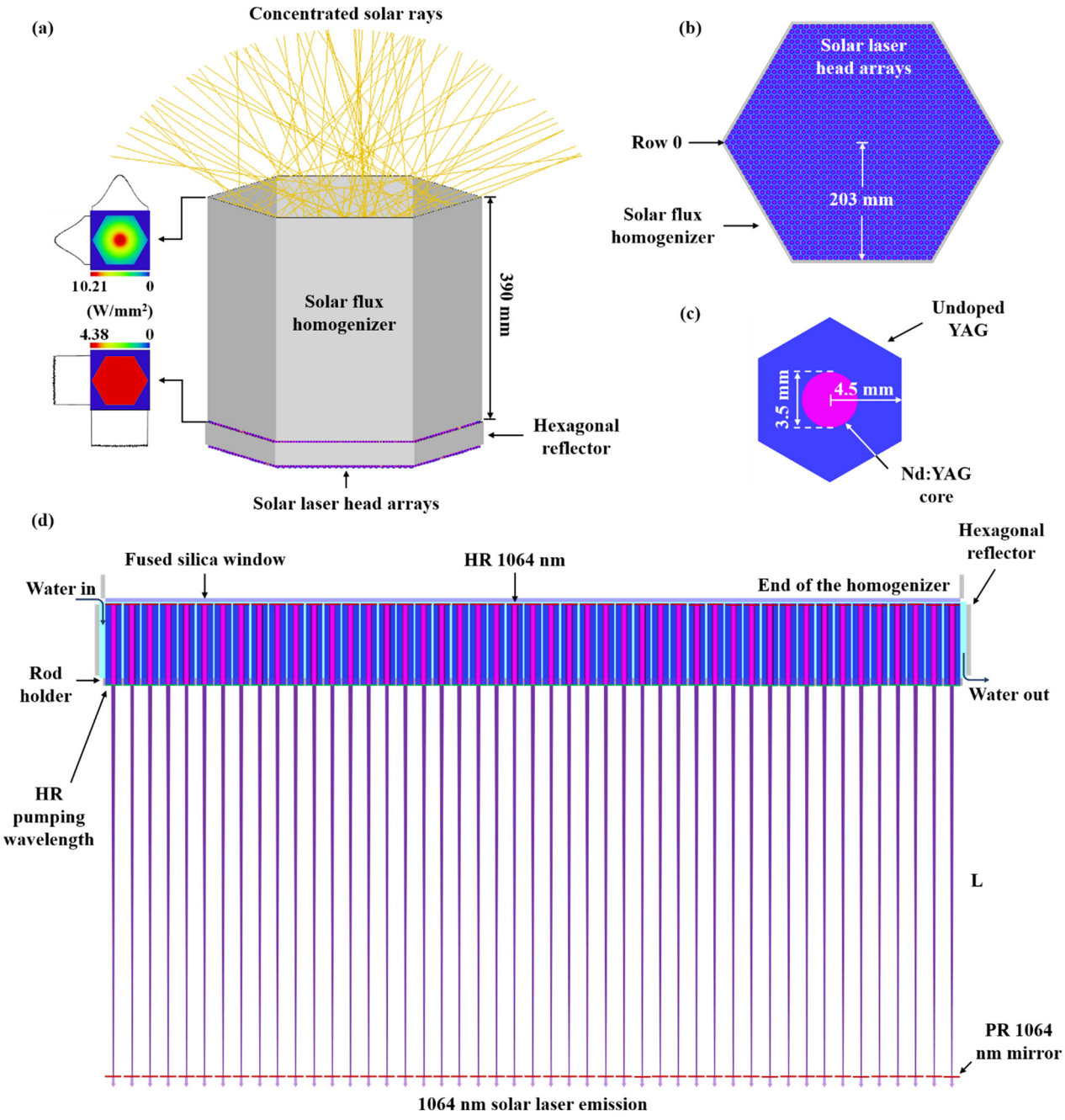

Figure 3. (**a**) 3D and (**b**) top view of the solar flux homogenizer, 1657 laser rods and the hexagonal reflector. The concentrated light distribution at the input and output faces of the homogenizer is also presented in (**a**). (**c**) Top view of a core-doped Nd:YAG rod. (**d**) Cross-sectional view of the lower part of the system, showing the central row (row 0, represented in (**b**)) with 47 solar laser rods, and the extraction of a laser beam from each one. L represents the separation length between the highly reflective (HR) at pumping wavelength coating on the lower end face of the rod and the partially reflective (PR) at 1064 nm output mirror.

Below the fused silica window, 1657 core-doped Nd:YAG laser rods were mounted vertically (Figure 3b,d), totaling 47 rows with different number of rods. Each rod had a 45 mm length and was composed of a cylindrical Nd:YAG core with a 3.5 mm diameter, and a hexagonal undoped YAG cladding with a 4.5 mm apothem (Figure 3c). With both homogenizer and undoped YAG claddings being hexagonal shaped, the rods could be

uniformly tiled on a flat plane with minimal gap losses. Surrounding the rods was a hexagonal reflector with a 206 mm apothem, 39 mm length, and 98% reflectivity for its inner walls. A single rod holder was used for mechanical fixation of the lower end of all core-doped Nd:YAG rods. The rods, the lower face of the fused silica window and the inner walls of the hexagonal reflector were water cooled, entering from the space between the fused silica window and the reflector, and exiting from the one between the rod holder and that same reflector. The cooling water helped in handling the temperature regulation because of its high thermal conductivity, as well as specific heat and low viscosity.

For the extraction of a laser beam, a highly reflective (HR) at the laser emission wavelength (1064 nm) coating was added to the top surface of each core-doped Nd:YAG rod. This coating, the laser rod and a partially reflective (PR) at 1064 nm output mirror constituted the laser resonator. The lower surface of each laser rod had a HR at pumping wavelength coating to help maximize the pump power.

3. Numerical Modeling of the Multibeam Solar Laser Station

3.1. Modeling of the Optical Design Parameters through Zemax® Software

For the optimization of the design parameters in Zemax®, a 1000 W/m^2 solar irradiance, typical during clear sunny days in Odeillo, France, was considered in the analysis. 22 peak absorption wavelengths for the 1.0 at. % Nd:YAG medium were programmed and the spectral irradiance values at each one were used as reference data for the light source, after consulting the standard solar spectrum for AM1.5 [49]. These spectral peaks were positioned at 527 nm, 531 nm, 568 nm, 578 nm, 586 nm, 592 nm, 732 nm, 736 nm, 743 nm, 746 nm, 753 nm, 758 nm, 790 nm, 793 nm, 803 nm, 805 nm, 808 nm, 811 nm, 815 nm, 820 nm, 865 nm, and 880 nm. Each peak wavelength and the corresponding absorption coefficient were also added to the glass catalog data of Zemax® for the Nd:YAG material. The parameters of the light source were first adjusted until a Gaussian profile, identical to that from the MWSF [48], was obtained at the focal spot (inset of Figure 3a). After that, the 16% overlap between the absorption spectrum of the Nd:YAG medium and the solar spectrum [50] was considered when estimating its effective pump power for the numerical analysis of the absorbed pump flux power and distribution within the core-doped Nd:YAG rods. Furthermore, the absorption spectra and wavelength-dependent refractive indices of fused silica and water were added to the glass catalog data of Zemax® to account for absorption losses in those media.

For the analysis of the numerical data within each rod, a detector volume, divided into several voxels, was necessary. The absorbed pump power was obtained through the sum of the power from each individual voxel. The number of analysis rays and voxels were tuned to acquire more accurate results and better image resolution of the detector. Figure 4 shows the absorbed pump flux distribution profiles in the longitudinal and four transversal cross-sections of one of the core-doped Nd:YAG laser media. The red color represents maximum pump flux of 0.25 W/mm^3, while blue is attributed to the laser rod regions where there is little or no absorption.

Due to the presence of the solar flux homogenizer, each core-doped rod exhibited absorbed pump flux distribution profiles similar to the ones in Figure 4, with the highest values being detected near the upper end face of the rod. Two regions of higher absorbed pump flux are present here, with a significant decline occurring between them as a result of the refraction of solar rays at the water/YAG and YAG/Nd:YAG interfaces. In addition, an increase of the absorbed pump flux with the distance to the rod's optical axis can be observed in the transversal cross-section profiles.

The absorbed pump flux data obtained from Zemax® were then processed in the LASCAD™ software in order to optimize the solar laser output power associated with the resonator beam parameters. The design parameters of the scheme were further optimized in Zemax® based on these results.

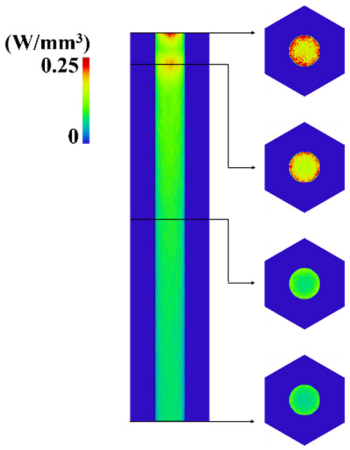

Figure 4. Absorbed pump flux distribution in the longitudinal and four transversal cross-sections of one core-doped Nd:YAG rod.

3.2. Optimization of the TEM_{00}-Mode Laser Extraction from Each Core-Doped Nd:YAG Medium through LASCAD™ Software

For the LASCAD™ analysis, a 2.8×10^{-19} cm^2 stimulated emission cross-section, a 230 µs fluorescence lifetime [18], and a 0.003 cm^{-1} typical absorption and scattering loss for the 1.0 at. % Nd:YAG medium were implemented. Moreover, the mean absorbed and intensity-weighted solar pump wavelength of 660 nm was considered [21].

The thermal induced effects in the 3.5 mm diameter, 45 mm length Nd:YAG cores were numerically analyzed in LASCAD™. Figure 5 shows an example of the thermal performance of one of the Nd:YAG cores. Maximum heat load of 0.14 W/mm^3 was attained, as well as a temperature of 306.2 K. A 8.87 N/mm^2 maximum stress intensity was also observed, which is significantly lower than the Nd:YAG material's stress fracture limit of about 200 N/mm^2 [51]. Therefore, the rods would perform relatively well under highly intense solar pumping.

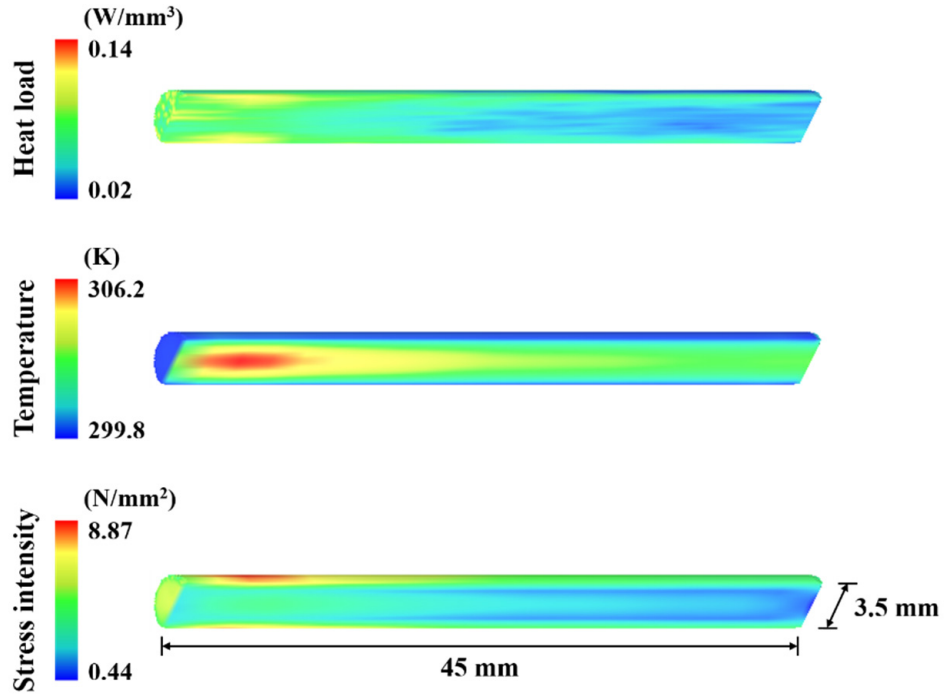

Figure 5. LASCAD™ analysis of heat load, temperature, and stress intensity distribution in one of the Nd:YAG cores.

Each laser resonator was composed of two opposing mirrors, representing the HR 1064 nm coating and the PR 1064 nm output mirror, whose optical axes were aligned with that of the laser rod. A PR mirror reflectivity of 97% provided the maximum TEM_{00}-mode laser power.

When the pump power exerts strong influence on the laser rod's thermal lens, the resonator length plays a crucial role in maximizing the extraction of TEM_{00}-mode laser beams with high brightness. In a resonator, the smallest size and divergence of a laser beam is obtained by its fundamental transverse mode [18]. For short resonators, the TEM_{00}-mode poorly matches the active region and laser oscillates in several modes, which leads to high M^2 factors. With the increase of the resonator length, the size of the TEM_{00}-mode beam within the rod also increases, as well as diffraction losses at the rod edges. Consequently, higher order modes can be eliminated. A long resonator was then chosen, to the detriment of laser power, so that only the fundamental mode could oscillate, improving the beam quality and, thus, its brightness [18]. To facilitate the oscillation of TEM_{00}-mode, a laser rod of small diameter had to be used since it behaves as an aperture. The separation length and the radius of curvature (RoC) of the PR mirror were also optimized. Figure 6 depicts the laser resonator design for one of the Nd:YAG cores to extract a TEM_{00}-mode laser beam.

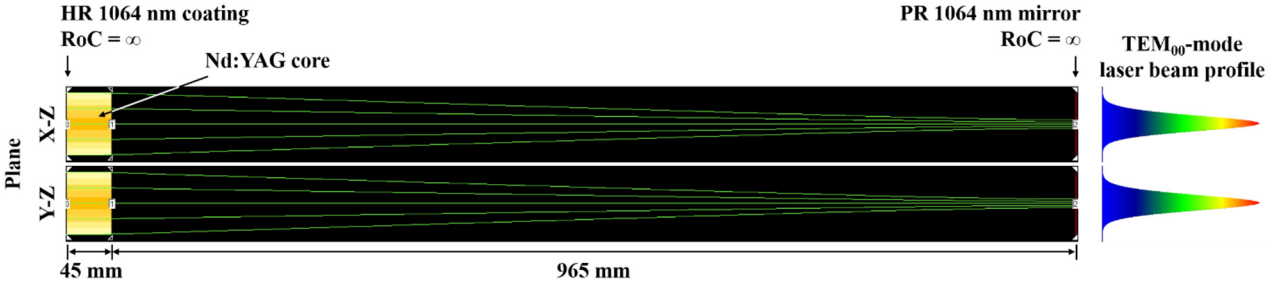

Figure 6. Laser resonator design in LASCAD™ for the extraction of a TEM_{00}-mode laser beam from one 3.5 mm diameter, 45 mm length Nd: YAG core. The beam profile is also presented.

In this end-side-pumping scheme, the thermal lensing effects were much less noticeable than in the previous 32-rod side-pumping concept with 6-mm diameter rods for the same solar furnace [38]. This made the use of thinner rods possible, which were pivotal in maximizing the TEM_{00}-mode laser power extraction with much longer resonant cavities. From each 3.5 mm diameter, 45 mm length Nd:YAG core, an average of 1.06 W TEM_{00}-mode solar laser power was numerically extracted, resulting in a total of about 1.8 kW. Each TEM_{00}-mode laser beam displayed good quality factors (M_x^2 = 1.29, M_y^2 = 1.02), albeit attaining a brightness of only 0.81 W. Total laser power of 15.2 kW in multimode regime was also numerically attained, with an average of 9.18 W from each individual rod, by reducing the resonant cavity length to 50 mm.

4. Extraction of Multiple TEM_{00}-Mode Laser Beams with Higher Brightness

By inclining each rod and positioning them at a certain distance from the fused silica window, a zigzag beam merging technique can be implemented to enable the extraction of brighter TEM_{00}-mode laser beams, despite having to reduce the number of rods. The angle of inclination of the rods should not be too low to avoid high laser beam transmission losses in the cooling water, since they would have to be positioned at a large distance from the fused silica window.

At approximately 7.62 mm below the fused silica window, 399 core-doped Nd:YAG laser rods were mounted at a 30° angle of inclination (Figure 7), which was the angle that also provided the highest absorbed pump power for each rod. This totals 35 rows with different number of rods, occupying almost the same space as the previous case of the laser beam extraction from each single rod. A wider hexagonal reflector surrounding the rods was adopted, with an apothem of 230 mm and length of 38.34 mm.

To extract a single laser beam from an array of core-doped rods, the resonant cavity was composed of a HR 1064 nm mirror, a certain number of rods (N), the fused silica window with a HR 1064 nm coating on its lower face, a set of horizontal HR 1064 nm folding mirrors (the amount of which differ depending on N), and a PR 1064 nm output mirror. The optical axes of the HR and PR 1064 nm mirrors were aligned with those of the outmost laser rods, while each horizontal HR 1064 nm folding mirror was placed between the lower end faces of two adjacent rods. Furthermore, in this case, the upper end face of each rod presented an antireflective (AR) at 1064 nm coating to allow the transmission of the laser beam toward the HR 1064 nm coating on the lower face of the fused silica window. The latter and the horizontal HR 1064 nm mirrors were essential in folding the laser light from one rod to the next one.

Considering the central row of the solar laser head as row 0, arrays with different N from this row were tested in order to determine which N led to the highest TEM_{00}-mode laser power production. For 3.5 mm diameter, 45 mm length Nd:YAG cores, N = 12 was the optimal number of rods, possibly generating 157.14 W of TEM_{00}-mode laser power. For this reason, N = 12 was used in every row that had at least this number of rods. For rows −17 to −9 and 9 to 17, the maximum N possible was used, varying from N = 8 to 11 rods. From the 399 rods, only 23 remained, positioned in rows −6 to 6, so they were split into two arrays of N = 10 and 13, employing a similar procedure for the extraction of the merged laser to those illustrated in Figure 7.

For the numerical analysis of the merged laser beam performance, a new method was adopted to acquire the text file with the absorbed pump flux/volume data to be imported into LASCAD™, because this software only allows the analysis of a single file. The following steps (Figure 8) were taken:

1. In Zemax®, a long detector volume was added for each of the N Nd:YAG cores of the array. Its length (L_{DET}) was N × L_{ROD}, with L_{ROD} being the rod length. The number of pixels in the *z*-axis was N × P_Z, with P_Z being the number of pixels from the previous case of laser beam extraction from each rod. Each Nd:YAG core occupied a different portion of the corresponding detector.
2. After running the Zemax® simulation, N text files were exported, with the absorbed pump flux/volume data from each detector volume.
3. Tables with information about each *z*-plane and voxel are crucial for the LASCAD™ analysis. Therefore, the lines with *z*-plane and voxel data from the different N text files were copied to replace the empty ones in the text file from one of the detectors. In Figure 8, the data from the detectors of rods 2 to 11 were used to replace the corresponding lines in the text file from rod 1 detector, since it already contained the absorbed pump flux/volume data of the Nd:YAG core in the detector volume's first portion. This helped in maintaining the same structure of a typical file directly exported from a detector volume in Zemax®. This single text file, with all the information of the core-doped Nd:YAG rods, was then imported into LASCAD™.

This resulted in a more compact laser resonator in LASCAD™ composed of the HR and PR 1064 nm mirrors, whose optical axes were aligned with that of the inclined laser rods 1 and 11, respectively, and a single laser rod with length equal to the sum of the lengths of each core-doped Nd:YAG rod of the array, as illustrated in Figure 9a for the merged laser beam of the N = 11 array in row 9. The total absorbed solar pump power for this single rod corresponded to the sum of the total pump power absorbed by each of the 11 rods. It is worth noting that the numerical analysis of the merged laser beams took into consideration the laser beam transmission losses (absorption, scattering, and diffraction) through both the Nd:YAG cores and the cooling water, as well as imperfections in the AR coatings on the end faces of the laser media and the HR coatings on the folding mirrors. For example, total round-trip loss of 32.2% was calculated for the merged TEM_{00}-mode laser beam from the N = 11 array in row 9, as shown in Figure 9a, resulting in maximum solar laser power of 153.69 W in fundamental mode regime (Figure 9b). M_x^2 = 1.12, M_y^2 = 1.01 laser beam quality factors were numerically found for this case. By using the beam propagation method in

LASCAD™, a near-Gaussian profile (Figure 9b) with beam waist radius of about 70.5 µm (Figure 9c) was numerically obtained at the PR 1064 nm output mirror, after several laser cavity iterations.

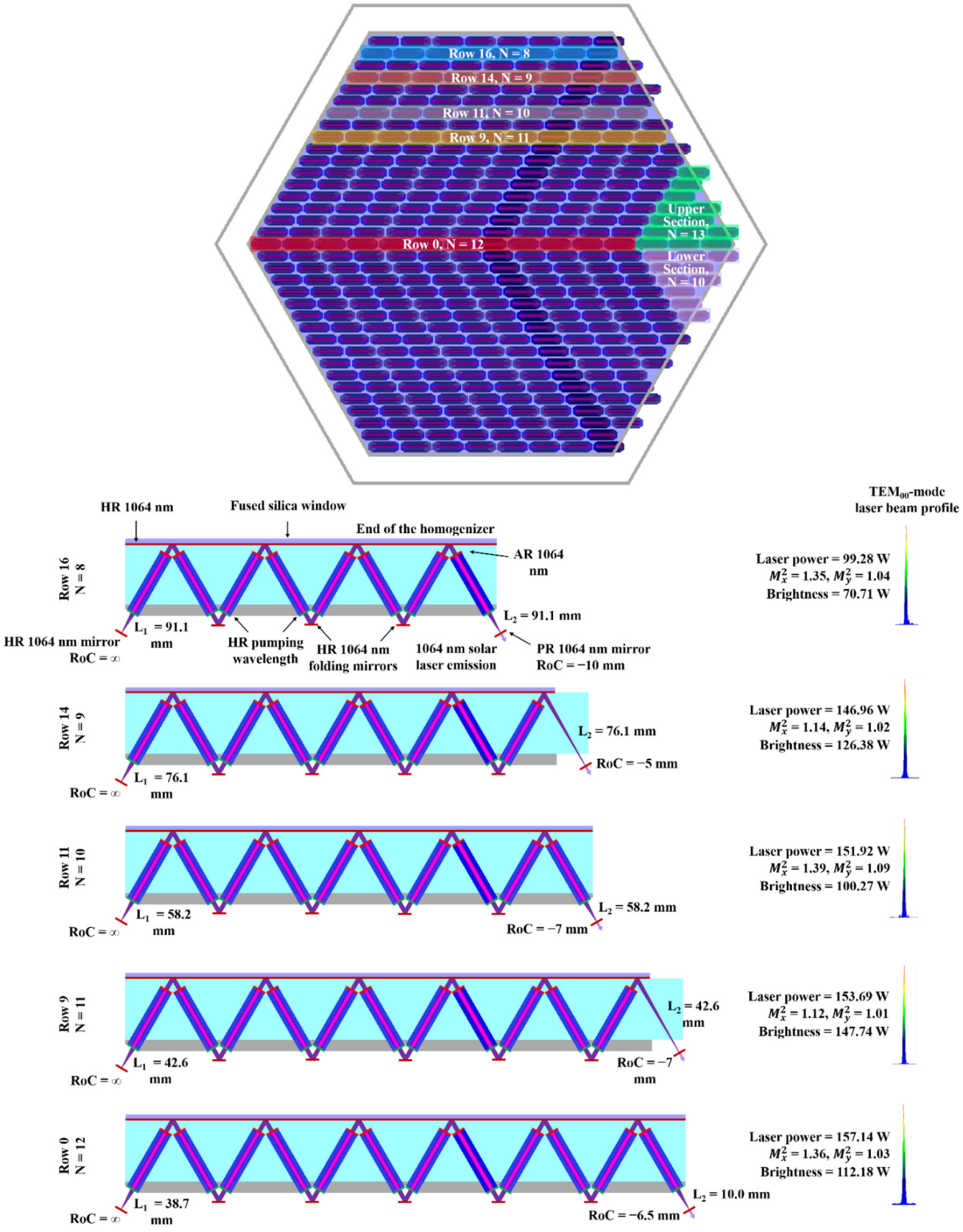

Figure 7. Illustration of the zigzag laser beam merging technique and TEM_{00}-mode laser performance for arrays of different N rods. L_1 is the separation length between the outer HR 1064 nm mirror and the lower end face of the leftmost rod, while L_2 represents the separation length between the lower or upper end face (determined by N) of the rightmost rod and the PR 1064 nm mirror. These separation lengths vary depending on N and the position of the array.

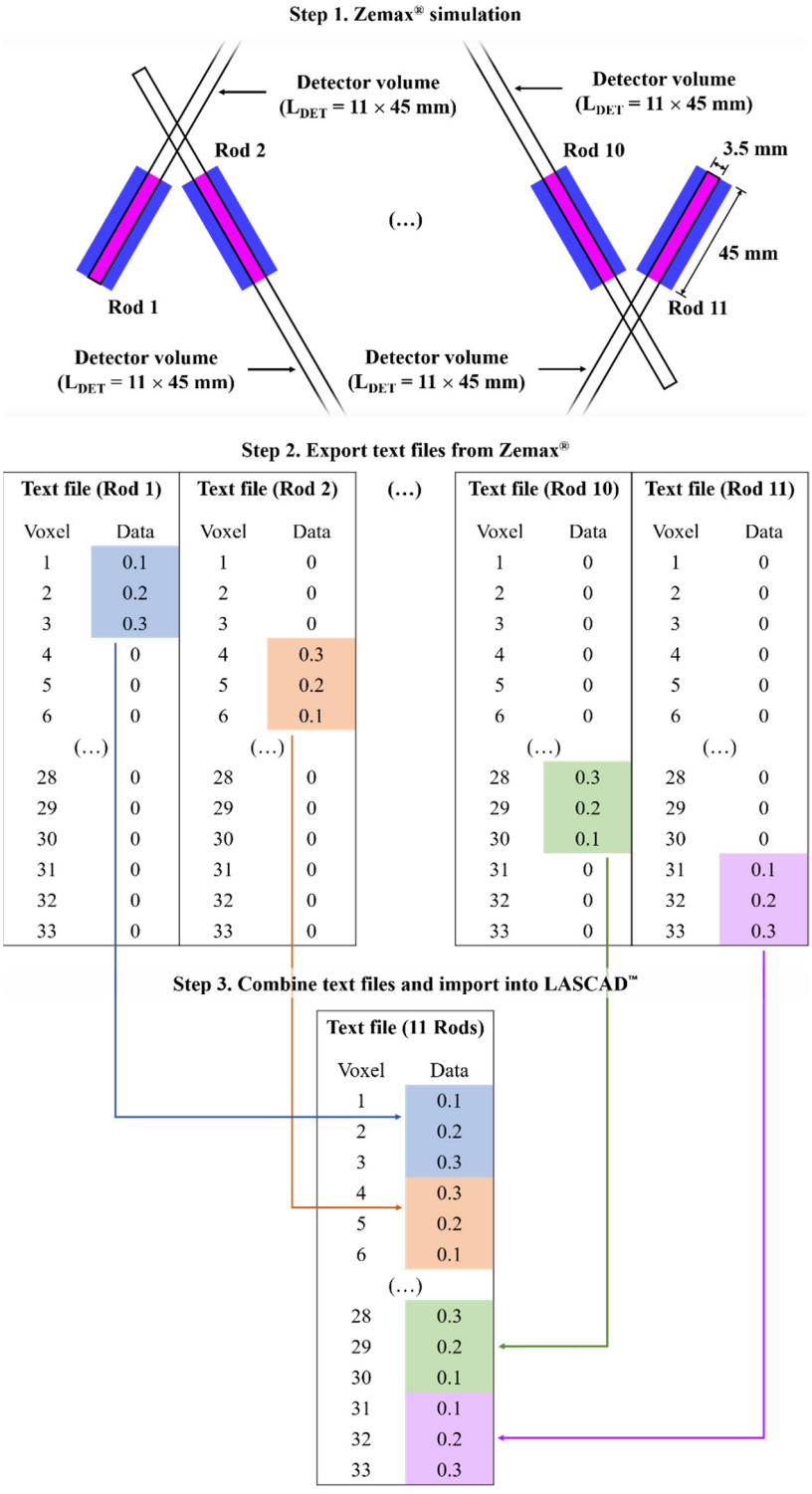

Figure 8. Simplified diagram of the process of combination of text files exported from Zemax® for LASCAD™ analysis of the extraction of a merged laser beam from an array with 11 rods. In this configuration, the HR and PR 1064 nm mirrors are closer to rod 1 and 11, respectively. The data presented in this diagram are for illustrative purposes only.

An analysis of the thermal induced effects on the N = 11 array of row 9 is presented in Figure 10. It shows that the maximum heat load (0.16 W/mm^3) and temperature (313 K) did not increase substantially in relation to the values observed with only a single Nd:YAG core.

The stress intensity (20.35 N/mm^2) rose over two times from the previously mentioned value, albeit still being considerably below the stress fracture limit of the Nd:YAG material.

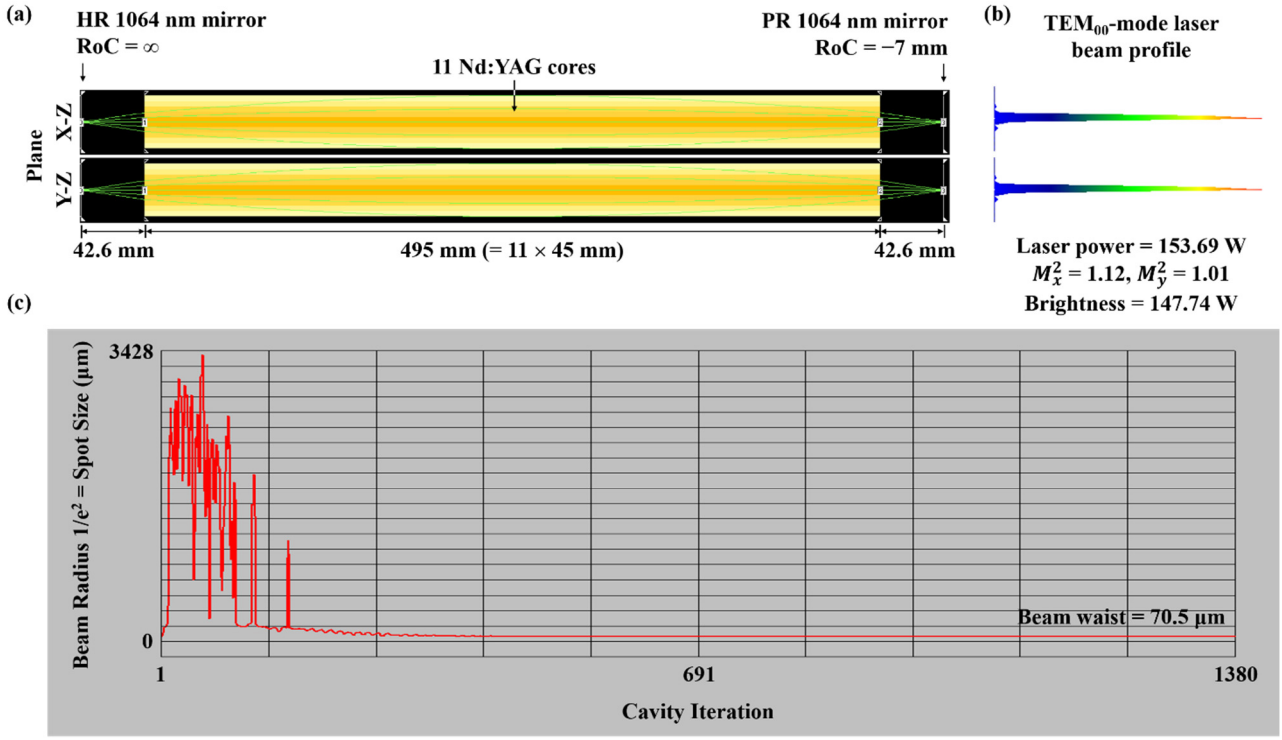

Figure 9. (**a**) Laser resonator design in LASCAD™ for the extraction of a merged TEM$_{00}$-mode laser beam from the N = 11 array of row 9, with (**b**) the respective beam profile. (**c**) Laser beam waist radius obtained at the PR 1064 nm output mirror, through the LASCAD™ beam propagation method.

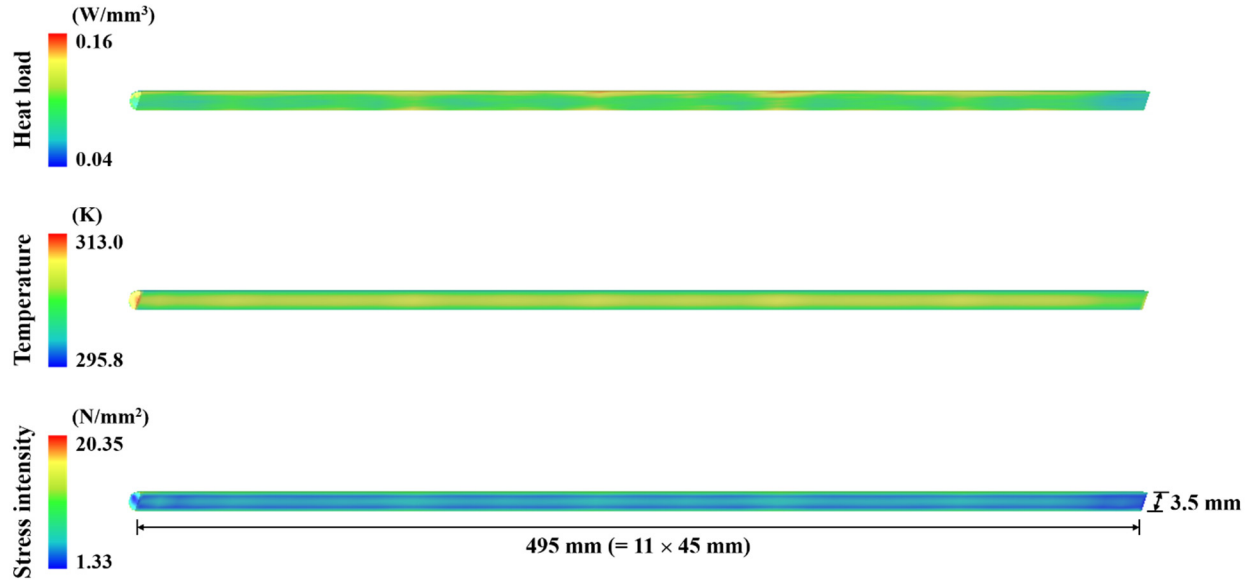

Figure 10. LASCAD™ analysis of heat load, temperature and stress intensity distribution in the N = 11 array of row 9.

The TEM$_{00}$-mode laser performance for five arrays of different N is detailed in Figure 7. With the laser beam merging technique, Gaussian laser beams of good quality with high TEM$_{00}$-mode power, and consequently, high brightness were attained, since it provided a better overlap between the pump and the fundamental mode volumes. Out of those five arrays, the N = 8 array of row 16 contributed with the lowest TEM$_{00}$-mode power of 99.28 W, which is 11.71 times greater than the 8.48 W total power from eight individual

TEM_{00}-mode laser beams (8 × 1.06 W). With the N = 12 array of row 0, the highest value of 157.14 W was obtained, corresponding to an increase of 12.35 times over the 12.72 W total power from twelve individual TEM_{00}-mode laser beams. The greatest enhancement, however, was achieved with the N = 9 array of row 14, which is 15.40 times higher than the 9.74 W total power from nine individual TEM_{00}-mode laser beams. The highest brightness figure of merit of 147.74 W was attained with the N = 11 array of row 9, which corresponds to a 182-fold increase over that from a single core-doped Nd:YAG rod. It is also 23 times higher than the experimental record of 6.46 W [16].

The TEM_{00}-mode and multimode laser power numerically extracted from each of the 37 arrays are presented in Figure 11. Despite the nearly uniform profile at the output end face of the homogenizer, a small difference in TEM_{00}-mode and multimode laser power from arrays with equal N was observed as a consequence of the position of certain rods that could not be placed in their entirety directly below the homogenizer's output face. Nevertheless, 5.2 kW total TEM_{00}-mode laser power may be extracted from 37 merged laser beams, corresponding to an improvement of three times in relation to the 1.8 kW attained before beam merging. Total multimode laser power of 8.6 kW was also determined.

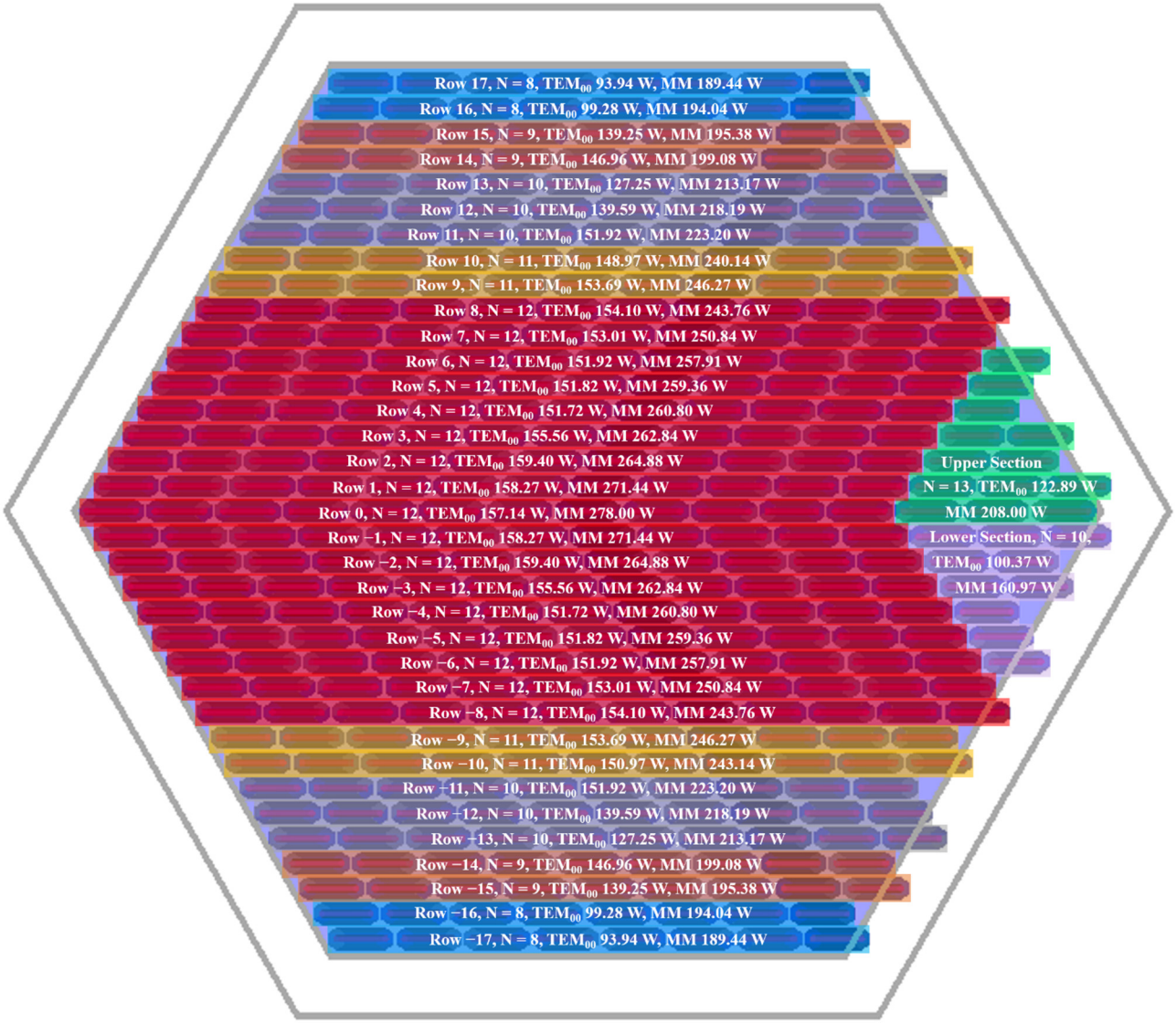

Figure 11. Summary of maximum TEM_{00}-mode (TEM_{00}) and multimode (MM) power attained from each laser beam extracted from different arrays of solar laser rods through the zigzag laser beam merging technique.

5. Conclusions

A multirod solar laser station concept was introduced to enable the production of high TEM_{00}-mode solar laser output power and beam brightness in MWSF. It was composed of a hexagonal shaped solar flux homogenizer with a fused silica window at its output end face, and 1657 core-doped Nd:YAG rods surrounded by a hexagonal reflector. The presence of the homogenizer facilitated the distribution of nearly the same amount of solar power to pump each rod and the substantial mitigation of the thermal lensing effects on each one, to the point that they were much less pronounced than in [38]. This facilitated the use of thin rods and long resonator cavities that are necessary to efficiently extract TEM_{00}-mode solar laser beams. With 3.5 mm diameter, 45 mm length Nd:YAG cores, a total laser power of 1.8 kW was numerically achieved.

The rod tilting and distance from the fused silica window may allow the possibility of employing a novel zigzag laser beam merging technique to boost the total TEM_{00}-mode solar laser output power and the beam brightness even further, despite having to reduce the number of rods from 1657 to 399. Not only was the TEM_{00}-mode power improved by three times, to 5.2 kW, from 37 merged laser beams, but the highest solar laser beam brightness figure of merit of about 148 W was also numerically determined, corresponding to a radical improvement of 23 times in relation to the previous experimental record [16]. The extraction of several high-power Gaussian TEM_{00}-mode solar laser beams of good quality and, thus, high brightness could greatly decrease the production costs with high-power lasers, paving the way for the future application of this renewable energy system in the industrial sector, as well as its expansion worldwide.

Author Contributions: Conceptualization, D.L., H.C., and J.A.; methodology, H.C., D.L., J.A. and C.R.V.; software, H.C., J.A., D.L., M.C. and B.D.T; validation, H.C., J.A. and D.L.; formal analysis, H.C., J.A., D.L. and D.G.; investigation, H.C., J.A. and D.L.; resources, D.L. and J.A.; data curation, H.C., J.A. and D.L.; writing—original draft preparation, H.C.; writing—review and editing, H.C., J.A., D.L., M.C., D.G., B.D.T. and C.R.V.; visualization, H.C.; supervision, D.L. and J.A.; project administration, D.L.; funding acquisition, D.L. All authors have read and agreed to the published version of the manuscript.

Funding: This research was funded by Fundação para a Ciência e a Tecnologia–Ministério da Ciência, Tecnologia e Ensino Superior, grant number UIDB/00068/2020.

Institutional Review Board Statement: Not applicable.

Informed Consent Statement: Not applicable.

Data Availability Statement: Not applicable.

Acknowledgments: The contract CEECIND/03081/2017 and the fellowship grants SFRH/BD/145322/2019, PD/BD/142827/2018, PD/BD/128267/2016 and SFRH/BPD/125116/2016 of Joana Almeida, Miguel Catela, Dário Garcia, Bruno D. Tibúrcio and Cláudia R. Vistas, respectively, are acknowledged.

Conflicts of Interest: The authors declare no conflict of interest. The funders had no role in the design of the study; in the collection, analyses, or interpretation of data; in the writing of the manuscript, or in the decision to publish the results.

References

1. Lando, M.; Kagan, J.A.; Shimony, Y.; Kalisky, Y.Y.; Noter, Y.; Yogev, A.; Rotman, S.R.; Rosenwaks, S. Solar-pumped solid state laser program. In Proceedings of the 10th Meeting on Optical Engineering in Israel, Jerusalem, Israel, 22 September 1997; Shladov, I., Rotman, S.R., Eds.; International Society for Optics and Photonics: Bellingham, WA, USA, 1997; Volume 3110, p. 196. [CrossRef]
2. Hemmati, H.; Biswas, A.; Djordjevic, I.B. Deep-Space Optical Communications: Future Perspectives and Applications. *Proc. IEEE* **2011**, *99*, 2020–2039. [CrossRef]
3. Rather, J.D.G.; Gerry, E.T.; Zeiders, G.W. Investigation of possibilities for solar powered high energy lasers in space. *NASA Tech. Rep. Serv.* **1977**. Available online: https://ntrs.nasa.gov/search.jsp?R=19770019534 (accessed on 15 March 2020).
4. Vasile, M.; Maddock, C.A. Design of a formation of solar pumped lasers for asteroid deflection. *Adv. Sp. Res.* **2012**, *50*, 891–905. [CrossRef]

5. Yabe, T.; Uchida, S.; Ikuta, K.; Yoshida, K.; Baasandash, C.; Mohamed, M.S.; Sakurai, Y.; Ogata, Y.; Tuji, M.; Mori, Y.; et al. Demonstrated fossil-fuel-free energy cycle using magnesium and laser. *Appl. Phys. Lett.* **2006**, *89*, 261107. [CrossRef]
6. Graydon, O. A sunny solution. *Nat. Photonics* **2007**, *1*, 495–496. [CrossRef]
7. Oliveira, M.; Liang, D.; Almeida, J.; Vistas, C.R.; Gonçalves, F.; Martins, R. A path to renewable Mg reduction from MgO by a continuous-wave Cr:Nd:YAG ceramic solar laser. *Sol. Energy Mater. Sol. Cells* **2016**, *155*, 430–435. [CrossRef]
8. Kiss, Z.J.; Lewis, H.R.; Duncan, R.C., Jr. Sun Pumped Continuous Optical Maser. *Appl. Phys. Lett.* **1963**, *2*, 93–94. [CrossRef]
9. Lando, M.; Kagan, J.; Linyekin, B.; Dobrusin, V. A solar-pumped Nd:YAG laser in the high collection efficiency regime. *Opt. Commun.* **2003**, *222*, 371–381. [CrossRef]
10. Yabe, T.; Ohkubo, T.; Uchida, S.; Yoshida, K.; Nakatsuka, M.; Funatsu, T.; Mabuti, A.; Oyama, A.; Nakagawa, K.; Oishi, T.; et al. High-efficiency and economical solar-energy-pumped laser with Fresnel lens and chromium codoped laser medium. *Appl. Phys. Lett.* **2007**, *90*, 261120. [CrossRef]
11. Liang, D.; Almeida, J. Highly efficient solar-pumped Nd:YAG laser. *Opt. Express* **2011**, *19*, 26399. [CrossRef]
12. Dinh, T.H.; Ohkubo, T.; Yabe, T.; Kuboyama, H. 120 watt continuous wave solar-pumped laser with a liquid light-guide lens and an Nd:YAG rod. *Opt. Lett.* **2012**, *37*, 2670. [CrossRef]
13. Xu, P.; Yang, S.; Zhao, C.; Guan, Z.; Wang, H.; Zhang, Y.; Zhang, H.; He, T. High-efficiency solar-pumped laser with a grooved Nd:YAG rod. *Appl. Opt.* **2014**, *53*, 3941. [CrossRef]
14. Guan, Z.; Zhao, C.; Li, J.; He, D.; Zhang, H. 32.1 W/m^2 continuous wave solar-pumped laser with a bonding Nd:YAG/YAG rod and a Fresnel lens. *Opt. Laser Technol.* **2018**, *107*, 158–161. [CrossRef]
15. Liang, D.; Vistas, C.R.; Tibúrcio, B.D.; Almeida, J. Solar-pumped Cr:Nd:YAG ceramic laser with 6.7% slope efficiency. *Sol. Energy Mater. Sol. Cells* **2018**, *185*, 75–79. [CrossRef]
16. Liang, D.; Almeida, J.; Vistas, C.R.; Guillot, E. Solar-pumped Nd:YAG laser with 31.5 W/m^2 multimode and 7.9 W/m^2 TEM$_{00}$-mode collection efficiencies. *Sol. Energy Mater. Sol. Cells* **2017**, *159*, 435–439. [CrossRef]
17. Hwang, I.H.; Lee, J.H. Efficiency and threshold pump intensity of CW solar-pumped solid-state lasers. *IEEE J. Quantum Electron.* **1991**, *27*, 2129–2134. [CrossRef]
18. Koechner, W. *Solid-State Laser Engineering*, 5th ed.; Springer Series in Optical Sciences; Springer: Berlin/Heidelberg, Germany, 1999; ISBN 978-3-662-14221-9.
19. Clarkson, W.A. Thermal effects and their mitigation in end-pumped solid-state lasers. *J. Phys. D. Appl. Phys.* **2001**, *34*, 2381–2395. [CrossRef]
20. Lupei, V.; Lupei, A.; Gheorghe, C.; Ikesue, A. Emission sensitization processes involving Nd^{3+} in YAG. *J. Lumin.* **2016**, *170*, 594–601. [CrossRef]
21. Weksler, M.; Shwartz, J. Solar-pumped solid-state lasers. *IEEE J. Quantum Electron.* **1988**, *24*, 1222–1228. [CrossRef]
22. Ostermeyer, M.; Brandenburg, I. Simulation of the extraction of near diffraction limited Gaussian beams from side pumped core doped ceramic Nd:YAG and conventional laser rods. *Opt. Express* **2005**, *13*, 10145. [CrossRef]
23. Sträßer, A.; Ostermeyer, M. Improving the brightness of side pumped power amplifiers by using core doped ceramic rods. *Opt. Express* **2006**, *14*, 6687. [CrossRef]
24. Almeida, J.; Liang, D. Design of a high brightness solar-pumped laser by light-guides. *Opt. Commun.* **2012**, *285*, 5327–5333. [CrossRef]
25. Liang, D.; Almeida, J. Design of ultrahigh brightness solar-pumped disk laser. *Appl. Opt.* **2012**, *51*, 6382. [CrossRef]
26. Liang, D.; Almeida, J. Multi-Fresnel lenses pumping approach for improving high-power Nd:YAG solar laser beam quality. *Appl. Opt.* **2013**, *52*, 5123. [CrossRef]
27. Garcia, D.; Liang, D.; Almeida, J. Core-doped Nd:YAG disk solar laser uniformly pumped by six Fresnel lenses. In Proceedings of the 8th Iberoamerican Optics Meeting and 11th Latin American Meeting on Optics, Lasers, and Applications, Porto, Portugal, 18 November 2013; Martins Costa, M.F.P.C., Ed.; International Society for Optics and Photonics: Bellingham, WA, USA, 2013; Volume 8785, p. 87850W. [CrossRef]
28. Strite, T.; Gusenko, A.; Grupp, M.; Hoult, T. Multiple Laser Beam Material Processing. *Biul. Inst. Spaw.* **2016**, *60*, 30–33. [CrossRef]
29. Eifel, S.; Holtkamp, J. Multi-Beam Technology Boosts Cost Efficiency. Available online: https://www.industrial-lasers.com/micromachining/article/16485583/multibeam-technology-boosts-cost-efficiency (accessed on 17 May 2020).
30. Gillner, A.; Finger, J.; Gretzki, P.; Niessen, M.; Bartels, T.; Reininghaus, M. High Power Laser Processing with Ultrafast and Multi-Parallel Beams. *J. Laser Micro/Nanoeng.* **2019**, *14*, 129–137. [CrossRef]
31. Olsen, F.O.; Hansen, K.S.; Nielsen, J.S. Multibeam fiber laser cutting. *J. Laser Appl.* **2009**, *21*, 133–138. [CrossRef]
32. Fazilov, A.; Riskiev, T.T.; Abdurakhmanov, A.A.; Bakhramov, S.A.; Makhkamov, S.; Mansurov, M.M.; Mukhamediev, E.J.; Paiziev, S.D.; Klychev, S.I.; Saribaev, A.S.; et al. Concentrated solar energy conversion to powerful laser radiation on neodymium activated yttrium-aluminum garnet. *Appl. Sol. Energy* **2008**, *44*, 93–96. [CrossRef]
33. Tibúrcio, B.D.; Liang, D.; Almeida, J.; Garcia, D.; Vistas, C.R. Dual-rod pumping concept for TEM$_{00}$-mode solar lasers. *Appl. Opt.* **2019**, *58*, 3438. [CrossRef] [PubMed]
34. Almeida, J.; Liang, D.; Tibúrcio, B.D.; Garcia, D.; Vistas, C.R. Numerical modeling of a four-rod pumping scheme for improving TEM$_{00}$-mode solar laser performance. *J. Photonics Energy* **2019**, *9*, 1. [CrossRef]
35. Liang, D.; Almeida, J.; Garcia, D.; Tibúrcio, B.D.; Guillot, E.; Vistas, C.R. Simultaneous solar laser emissions from three Nd:YAG rods within a single pump cavity. *Sol. Energy* **2020**, *199*, 192–197. [CrossRef]

36. Costa, H.; Almeida, J.; Liang, D.; Garcia, D.; Catela, M.; Tibúrcio, B.D.; Vistas, C.R. Design of a multibeam solar laser station for a megawatt solar furnace. *Opt. Eng.* **2020**, *59*, 086103. [CrossRef]
37. Almeida, J.; Liang, D.; Costa, H.; Garcia, D.; Tibúrcio, B.D.; Catela, M.; Vistas, C.R. Seven-rod pumping concept for simultaneous emission of seven TEM_{00}-mode solar laser beams. *J. Photonics Energy* **2020**, *10*, 038001. [CrossRef]
38. Costa, H.; Almeida, J.; Liang, D.; Tibúrcio, B.D.; Garcia, D.; Catela, M.; Vistas, C.R. Quasi-Gaussian Multibeam Solar Laser Station for a Megawatt Solar Furnace. *J. Sol. Energy Res. Updat.* **2021**, *8*, 11–20. [CrossRef]
39. Liang, D.; Almeida, J.; Tibúrcio, B.D.; Catela, M.; Garcia, D.; Costa, H.; Vistas, C.R. Seven-Rod Pumping Approach for the Most Efficient Production of TEM_{00} Mode Solar Laser Power by a Fresnel Lens. *J. Sol. Energy Eng.* **2021**, *143*, 061004. [CrossRef]
40. Liang, D.; Almeida, J. Solar-Pumped TEM_{00} Mode Nd:YAG laser. *Opt. Express* **2013**, *21*, 25107. [CrossRef] [PubMed]
41. Liang, D.; Almeida, J.; Vistas, C.R.; Guillot, E. Solar-pumped TEM_{00} mode Nd:YAG laser by a heliostat-Parabolic mirror system. *Sol. Energy Mater. Sol. Cells* **2015**, *134*, 305–308. [CrossRef]
42. Almeida, J.; Liang, D.; Vistas, C.R.; Bouadjemine, R.; Guillot, E. 5.5 W continuous-wave TEM_{00}-mode Nd:YAG solar laser by a light-guide/2V-shaped pump cavity. *Appl. Phys. B* **2015**, *121*, 473–482. [CrossRef]
43. Vistas, C.R.; Liang, D.; Almeida, J. Solar-pumped TEM_{00} mode laser simple design with a grooved Nd:YAG rod. *Sol. Energy* **2015**, *122*, 1325–1333. [CrossRef]
44. Liang, D.; Almeida, J.; Vistas, C.R.; Oliveira, M.; Gonçalves, F.; Guillot, E. High-efficiency solar-pumped TEM_{00}-mode Nd:YAG laser. *Sol. Energy Mater. Sol. Cells* **2016**, *145*, 397–402. [CrossRef]
45. Duocastella, M.; Arnold, C.B. Bessel and annular beams for materials processing. *Laser Photonics Rev.* **2012**, *6*, 607–621. [CrossRef]
46. Catela, M.; Liang, D.; Vistas, C.R.; Garcia, D.; Tibúrcio, B.D.; Costa, H.; Almeida, J. Six-rod/six-beam concept for revitalizing TEM_{00} mode lamp-pumped lasers. *Opt. Eng.* **2020**, *59*, 126108. [CrossRef]
47. Guillot, E.; Rodriguez, R.; Boullet, N.; Sans, J.-L. Some details about the third rejuvenation of the 1000 kWth solar furnace in Odeillo: Extreme performance heliostats. In Proceedings of the AIP Conference Proceedings; 2018; Volume 2033, p. 040016. Available online: https://aip.scitation.org/doi/abs/10.1063/1.5067052 (accessed on 24 August 2021). [CrossRef]
48. SFERA Access to PROMES Facilities. Available online: http://sfera.sollab.eu/index.php?page=access_promes (accessed on 6 May 2020).
49. ASTM G173-03(2012). *Standard Tables for Reference Solar Spectral Irradiances: Direct Normal and Hemispherical on 37° Tilted Surface*; ASTM: West Conshohocken, PA, USA, 2012. [CrossRef]
50. Zhao, B.; Changming, Z.; He, J.; Yang, S. The study of active medium for solar-pumped solid-state lasers. *Acta Opt. Sin.* **2007**, *27*, 1797–1801.
51. Almeida, J.; Liang, D.; Vistas, C.R.; Guillot, E. Highly efficient end-side-pumped Nd:YAG solar laser by a heliostat–parabolic mirror system. *Appl. Opt.* **2015**, *54*, 1970. [CrossRef] [PubMed]